INTERNATIONAL JOURNAL OF AUTOMOTIVE SCIENCE AND TECHNOLOGY

2025, VOL. 9, NO:3, 436-445 www.ijastech.org e-ISSN: 2587-0963

Prediction Performance of Low Error Rate Adaptive Fading Kalman Filter Due to Temperature Change

Eren Mehmet Akbaş[1*] and Murat Üçüncü[2]

[1] *TUBITAK (The Scientific and Technological Research Council of Turkey), Ankara, 06790, Turkey*
[2] *Electrical and Electronics Engineering Department, Faculty of Engineering, Başkent University, Ankara, 06790, Turkey*

Research Article

Abstract

Global Navigation Satellite System (GNSS) is a system which provides very accurate positioning information. The performance of GNSS depends on several factors such as propagation, interference, denial of full service etc. On the other side, inertial navigation system (INS) can work as a standalone system which does not require any external source support. The main problem in INS is the accumulation of error as time evolves. Apart from that , some inertial measurement units may be succeptible to noise and uncertainty in their output. When GNSS is not functional, it is necessary to have measures to increase the robustness of navigation algorithms and compensate for sensor errors when only INS is used. Additionally , temperature is another important factor that should be taken into account. The INS sensors' response to temperature changes may change and therefore adversely effect the estimation results. Otherwise, we can encounter problems in prediction algorithms to predict states accurately due to the accumulation of errors over time . In this study, we attempted to minimize errors due to measurements with different sensors by using a low-error-rate adaptive fading Kalman filter (LERAFKF). The simulation studies were carried out by using two different IMU's. One IMU is a temperature-sensitive SDI33 model inertial measurement unit (IMU). The second IMU is Honeywell HG9900C1A IMU sensor with 9 degrees of freedom and resistant to temperature change. The measurement set up has a 2-axis rotating head and a temperature control feature We have proved that LERAFKF provides a robust prediction against temperature changes with two different sensors.

Keywords: Adaptive fading Kalman Filter, IMU sensor temperature, Kalman Filter, State-Space model, Inertial measurement unit

History
Received 04.11.2024
Revised 13.06.2025
Accepted 15.09.2025

Contact
* Corresponding author
Murat Üçüncü
murat.ucuncu@yahoo.com.tr
Address: Başkent University, Department of Electrical and Electronics Engineering, Fatih Sultan Mahallesi, Bağlıca Kampüsü, 06790, Ankara,,Türkiye.
Tel: +903122464045

To cite this paper: Akbaş, E.M., Üçüncü, M., Prediction Performance of Low Error Rate Adaptive Fading Kalman Filter Due to Temperature Change. International Journal of Automotive Science and Technology. 2025; 9 (3): 436-445. https://doi.org/10.30939/ijastech..1578259

1. Introduction

Inertial Navigation System (INS) is a stand-alone sensor that can provide navigation at a high measurement rate without the need for any other external source. One of the main problems adversely affecting the performance of INS sensors is the temperature of the measurement system. This problem results in an increase in the navigation error over time [1].

Moreover, the intrinsic faults inherently available in MEMS (microelectronic mechanical system)-based inertial measurement units, such as constant shift, scale factor, bias and nonorthogonality, adversely affect such devices. As a result, their output may contain considerable noise and uncertainty [2]. Especially if the GNSS is disabled, some measures need to be taken to make the performance of navigation algorithms more robust and to compensate for the deficiency caused by sensor temperature changes [3]. Therefore, problems arise in prediction algorithms for predicting future states correctly due to the accumulation of errors with time [4].

The Kalman filter is very robust when the system parameters are known exactly. However, in some cases, the specifications of the system are not well characterized, which significantly affects the filter estimation performance [2-4].

In this context, the first study was carried out by R. E. Kalman [5] in 1960, and the first examples of the estimation problem emerged.

In 1971, R.K. Mehra [6] continued to work with the linear model, and many studies were carried out on correcting the errors that occurred in the KF between 1972 and 1999.

For the first time, the forgetting factor came to the fore in the studies conducted by Lee in 1988 [7] and by Xia [8] in 1994.

Studies on the system created as a result of the measurement taken with the IMU sensor gained momentum with Bar-Shalom [9] in 2001 and later by Titterton [2] in 2004.

Hide C. [10] conducted a study on velocity and acceleration estimation by using a Kalman filter, where he used a low-cost INS.

El-Sheimy N. [11] worked on modelling and analysis with an inertial sensor using the Allan variance method.

Ding W. [12] improved the estimation result with an integrated GNSS/INS model.

Gao B. [13] performed a robust adaptive filter design with tightly coupled GNSS/INS integration. In a similar study, Song J. [14] improved the estimation result with the help of a 3D magnetic vector in the case of GPS (Global Positioning System) disabled.

Zhang L. [15] proposed a robust adaptive Kalman filter mainly used in navigation systems in 2021.

Faragher R. [16] derived a new type of Kalman filter that includes two Gaussian functions and has a more compact form.

Bou S. [17] proposed the multiple fading factor Kalman filter algorithm, which involves a one-step prediction of the state estimation.

Finally, E. Akbaş et al. [18] developed a low error rate adaptive fading Kalman filter (LERAFKF) algorithm to predict the states of a state-space system in a robust way [18].

The most important issue in these studies is that when it is necessary to navigate only with the INS, the deviation can be minimised by making predictions with low error by using sensor outputs that may change with the ambient temperature and internal temperature, and this can be tested with an IMU sensor that is widely used today. In this study, the prediction performance of LERAFKF against sensor temperature changes was investigated.

2. Related Works

2.1 Kalman Filter Algorithm

The Kalman Filter is an iterative filter that estimates the state variables of the system and tries to converge to the true value. The Kalman Filter is a very successful and capable filter in estimating state variables. In this study, the system dynamics concerning state variables are considered for a discrete-time state-space system given by Eq. (1) and Eq.(2) [19-21].

$$x_{k+1} = \Phi_k \ x_k + G_k \ w_k \tag{1}$$

$$y_{k+1} = H_k \ x_{k+1} + \ v_{k+1}$$

(2)

Here, x is an n-dimensional vector, the state; w_k is a p vector, the disturbance; y is an m-dimensional vector, the measurement error; and k=0,1,2,……, is the discrete-time index. Φ_k is an nxn matrix, the state transition matrix; G_k is an nxp matrix, the disturbance transition matrix; and H_k is an mxn matrix, the measurement matrix. The process w_k is a p-dimensional Gaussian white noise sequence and v_k is an m-dimensional Gaussian white noise sequence.

The Kalman filter operates in a "predict-correct" fashion. The correction term involves a weighting of the mesaurement residual referred to as the weighting matrix, or the Kalman gain matrix. Kalman gain and recursive state estimates together with the error covariance matrix are summarised by Eq. (3)-Eq. (5) as given below [20].

The state estimation starts with the initial value x_0 and initial error covariance P_0. The description of the error covariance, the Kalman gain and the recursive state estimates are summarized by Eq. (3)-Eq. (5) as given below.

$$\hat{x}_{k+1/k+1} = \hat{x}_{k+1/k} + \ K_{k+1}(y_{k+1} - H_{k+1} \ \hat{x}_{k+1/k}) \tag{3}$$

$$P_{k+1/k} = \Phi_{k+1} \ P_{k/k}\Phi^T_{k+1/k} + G_{k+1} \ Q_k G^T_{k+1}$$

(4)

$$K_{k+1} = P_{k+1/k} \ H^T_{k+1}(H_{k+1} \ P_{k+1/k}H^T_{k+1} + R_{k+1}) \ ^{-1}$$

(5)

Here, $\hat{x}_k$ is the state estimate, P_k is the covariance matrix, Q_k is the state error covariance matrix [E(w(j)wT(k)]= Q_k] , R_k is the measurement noise covaraince [E(w(j)wT(k)] =R_k].

The details of the Kalman filter algorithm can be found in several literature [5,9,16,19]. We can see that the Kalman Gain is used as an input for the model to improve subsequent predictions. Here, we also see that the Kalman gain is adaptively changed [20]. KFs yield very good prediction results when the noise affecting the system parameters is statistically well-modelled [3,4]. However, since noise is time-, space- and sensor-dependent, it is not easy to determine when and how some changes occur [12]. If it is thought that there is a problem in system modelling, then relatively high values of Q should be chosen [22].

2.2 Adaptation of the Kalman Filter with a Low Error Rate Fading Factor

The Kalman filter works successfully if it accurately includes the dynamics of the system to be estimated. However, the use of incorrect prior values and unknowns due to temperature differences in the system and observation matrices will cause the predictions to be incorrect or even diverge during filter operation [21,22]. The goal of adaptive filters, which are required in these situations, is to reduce prediction error and address the divergence problem [21]. In this context, an algorithm named low-error-rate adaptive fading Kalman filter (LERAFKF) has been proposed by E. Akbaş et al. [18]. The proposed algorithm has a revised covariance matrix that includes a forgetting factor [18] and modifies Kalman filter by giving more weight to the most recent measurements as they are more useful for prediction [22]. In this context, the recommended LERAFKF has a revised covariance matrix including a forgetting factor. The covariance matrix of the error is weighted as defined in Eq. (6).

$$P_{k+1/k} = \lambda_k \Phi_{k+1} P_{k/k} \Phi'_{k+1/k} + G_{k+1} Q_k G'_{k+1} \quad (6)$$

Here, λ_k is the so-called forgetting factor. Indeed, the weighting factor is defined as the forgetting factor λ_k>1. We see that λ_k=1 gives us the standard KF covariance matrix. All the details about the calculation of the forgetting factor are given in [18, 23,24]. This method was developed and proposed by weighting the covariance matrix of the error in incorrectly constructed state space models and adding various update steps in addition to the estimation steps. It greatly minimizes the divergence and deviation problem as a result of inaccurate measurement. While doing this, it proceeds by weighting the new observation values added to the forecast against the old forecasts. This, of course, add an additional processing which can be negligible in terms of the processing power of today's technology.

3. Material and Method

In the simulation studies, we used two different IMUs and had the opportunity to test them in the same environment at 3 different temperatures.

The success of LERAFKF was demonstrated by using an SDI33 and HG90900C1A IMU system This measurement environment has a 2-axis rotating head and a temperature control feature. As seen in the test setup shown in Figure 1, axial rotations are provided by the operator using its own interface for the IMU mounted inside, and the temperature inside the cabin can be adjusted from low to high with a temperature change of 1 degree intervals per minute.

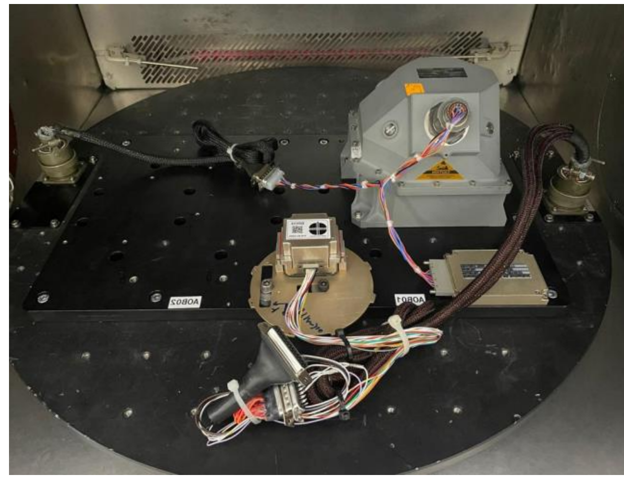

Figure 1. Test Setup for the HG9900C1A and SDI33 IMU Sensors

We tested the success of LERAFKF with a second-order system representing a moving object, which was also used in the study carried out by Bar-Shalom et al. [9]. For this purpose, we used a 2-axis rotary table installed in a missile measurement laboratory.

For measurement, we used the acceleration data taken with two different IMUs, model 9DOF SDI33 and model Honeywell HG9900C1A (with 9 degrees of freedom) which are part of this setup and placed on a 2-axis rotary table. SD133 Model IMU and HG9900C1A are shown in Figure 2.a and Figure 2.b, recursively.

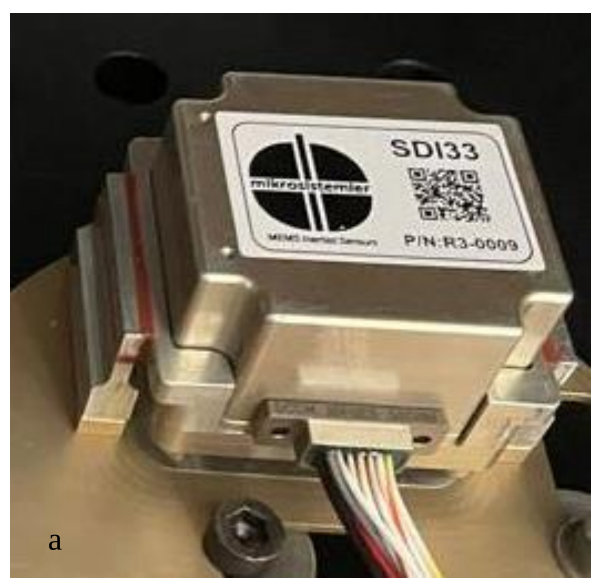

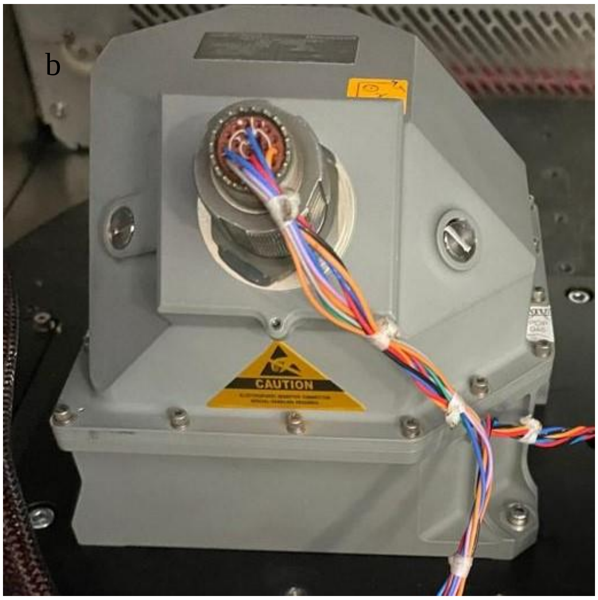

Figure 2.IMUs used in the study a) SD133 Model IMU b) HG9900C1A Model IMU

Detailed information on the sensor characteristics is given in Table 1 and Table 2.

Table 1. SDI33 Model IMU Characteristics and Performance

Standard Interface Protocol	200 Hz filtered angular rate and linear acceleration
Gyro Operating Range	± 350 °/sec
Accelerometer Operating Range	Standard: ± 17 g
Gyro Error Coefficients(1σ)	Bias: < 0.0091 °/HR Random Walk:<0.004 °/√HR Scale Factor: < 7.0 PPM"
Accelerometer Error Coefficients (1σ)	Bias: < 33µg Scale Factor: < 200 PPM
Optimal Thermal Operating Range	-25°C to +55°C
Input Voltage	12, ±35 Vdc input

The operating temperature range of the Model SD133 IMU sensor is -25o to 55o degrees Celsius. As seen here, the operating temperature range is 80 degrees. On the other hand, the HG9900C1A Model IMU can operate in a wider temperature range of 111 degrees, from -40o to 71o degrees. Moreover, as depicted in Figure 3, it is clear that the HG9900C1A is a more professional IMU sensor that is both ruggedized and high-quality military-grade sensor. HG9900C1A is currently used in military aircrafts.

Table 2. HG9900C1A Model IMU Characteristics and Performance

Standard Interface Protocol	SDLC RS-422 300 Hz filtered angular rate and linear acceleration (other frequencies available)
Gyro Operating Range	± 550 °/sec
Accelerometer Operating Range	Standard: ± 20 g Additional Options: ± 1.4 g, ± 30 g, ± 50 g, and ± 70 g
Gyro Error Coefficients(1σ)	Bias: < 0.0035 °/HR Random Walk: < 0.002 °/√HR Scale Factor: < 5.0 PPM"
Accelerometer Error Coefficients (1σ)	Bias: < 25µg Scale Factor: < 100 PPM
Optimal Thermal Operating Range	-40°C to +71°C
Input Voltage	5, ±15 Vdc input

The acceleration-time graphs of the measurements taken starting from -20°C and increasing by 1 degree up to +50°C show that the acceleration values of HG9900C1A are more resistant to temperature changes than those of SDI33, as depicted in Figure 3 and Figure 4, respectively. Furthermore, one can see that there was an offset in the acceleration of the SDI33 sensor on the X-axis at low temperature compared to that at high temperature, as shown in Figure 4. Specifically, the HG9900C1A model IMU is more resistant to temperature changes than the SDI33 model.

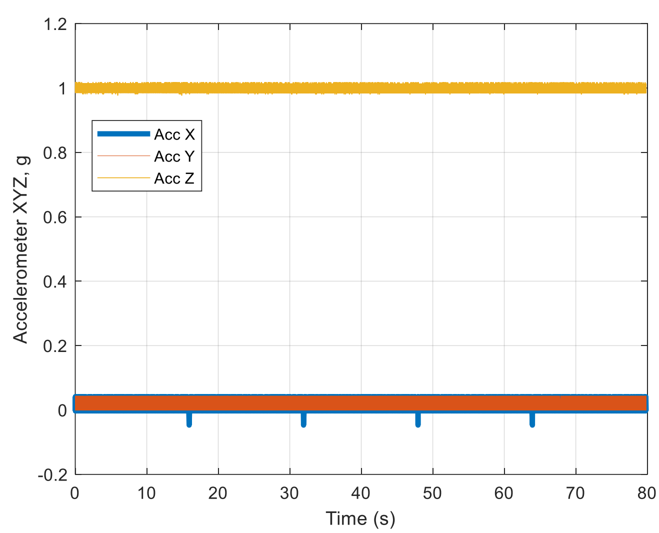

Figure 3. HG9900C1A IMU Sensor, -20°C - +50°C

Measurements were taken in a research center experimental environment. Different sample values obtained in the clockwise and counter-clockwise directions on the X-axis were used with the north orientation test taken for 3 different temperatures at -20°C, +20°C and +50°C.

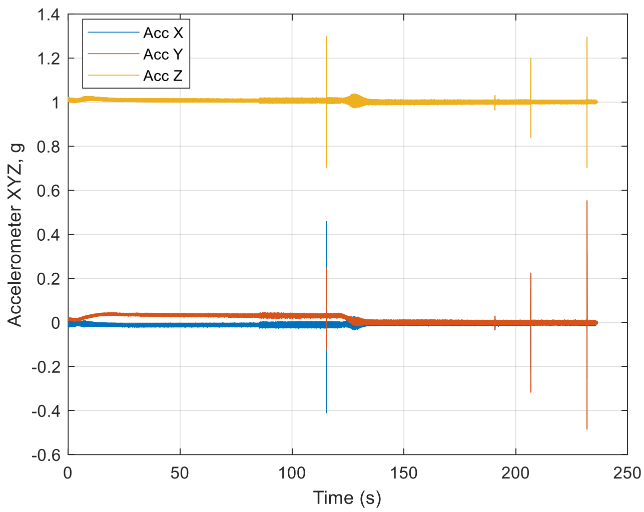

Figure 4. SDI33 IMU Sensor, -20°C - +50°C

The moving object dynamics in the discrete time domain are given by Eq. (7) and Eq. (8).

$$x_{k+1} = \begin{bmatrix} 1 & 1 \\ 0 & 1 \end{bmatrix} x_k + \begin{bmatrix} 0.5 \\ 1 \end{bmatrix} w_k \quad (7)$$

$$y_{k+1} = \begin{bmatrix} 1 & 0 \end{bmatrix} x_{k+1} + v_{k+1} \quad (8)$$

Here, the input and output disturbances are defined as Gaussian distributions with $w_k \sim N(0,1)$, $v_k \sim N(0,1)$, respectively, for noise processes and $x_0 = \begin{bmatrix} 0 \\ 10 \end{bmatrix}$ for the initial state.

We also analysed the system described by Eq. (9) and Eq. (10) by slightly distorting one parameter of the system discussed in the previous paragraph. Our aim here was to compare the performances of the Kalman filter and LERAFKF [18] systems when we use this deliberately distorted system.

$$x_{k+1} = \begin{bmatrix} 1 & 1 \\ 0 & 1.1 \end{bmatrix} x_k + \begin{bmatrix} 0.5 \\ 1 \end{bmatrix} w_k$$

(9)

$$y_{k+1} = \begin{bmatrix} 1 & 0 \end{bmatrix} x_{k+1} + v_{k+1} \quad (10)$$

Here, the input and output disturbances are defined the same as in the previous paragraph. In the measurement environment we used, the rotary table was adjusted so that the magnetic north was exactly 0 degrees, and by keeping this degree constant, the measurement environment cover was closed, and raw data were collected for 3 different temperatures at -20°C, +20°C and +50°C.

4. Simulation Studies

In the first study, the prediction performance of the Kalman filter was analysed when a linear model was used with data received from sensors at a +20°C sensor temperature. In the second study, the prediction performances of the Kalman filter and LERAFKF at the same temperature for cases where a parameter of the linear model is selected incorrectly are presented and compared. In the third study, the changes in the performances of the KF and LERAFKF prediction algorithms with respect to different sensor temperature ranges are tested and compared . In the simulation studies, the parameters of Q or R are not chosen incorrectly, but the output performance is analyzed by making various changes to them. The system parameter values were analyzed as inconsistent with the actual system dynamics. The false state space model was erroneously constructed due to incorrectly defined system dynamics.

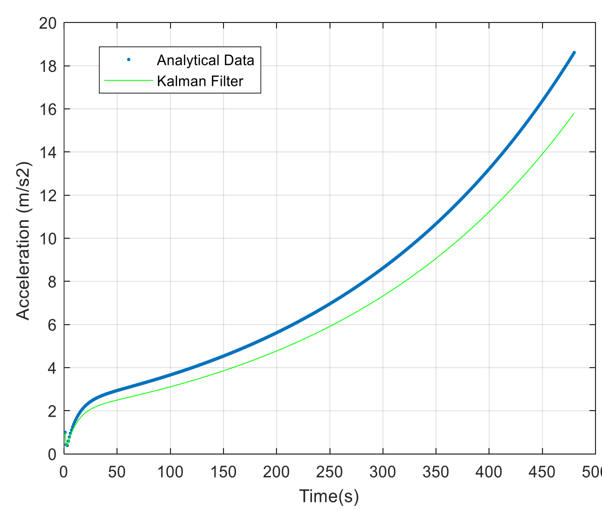

Figure 5. Unmeasured state (acceleration) value & Kalman Filter estimate

An important issue here is that it is also appropriate to look at the analytical value and the estimated values of the unmeasured state variables. First of all, the unmeasured acceleration value was estimated by Kalman Filter (Figure 5). When the LERAFKF algorithm is applied, the analytical value of the unmeasured state variable and the LERAFKF estimation value are given in Figure 6. As can be seen, LERAFKF performs much better than the Kalman algorithm for the unmeasured state variable.

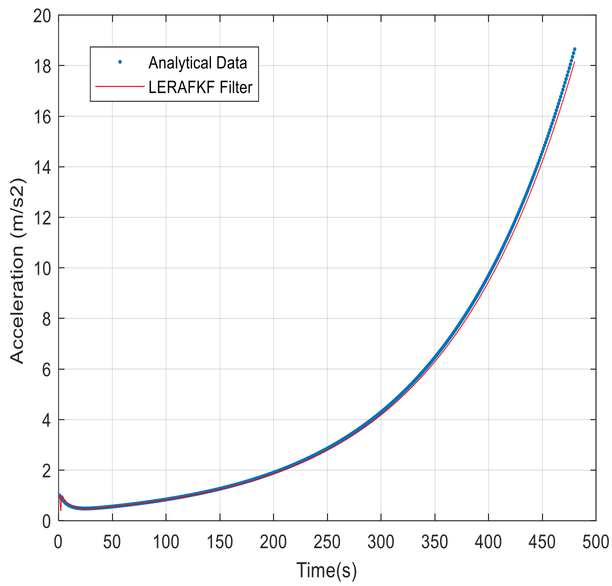

Figure 6. Unmeasured state (acceleration) value & LERAFKF Filter estimate

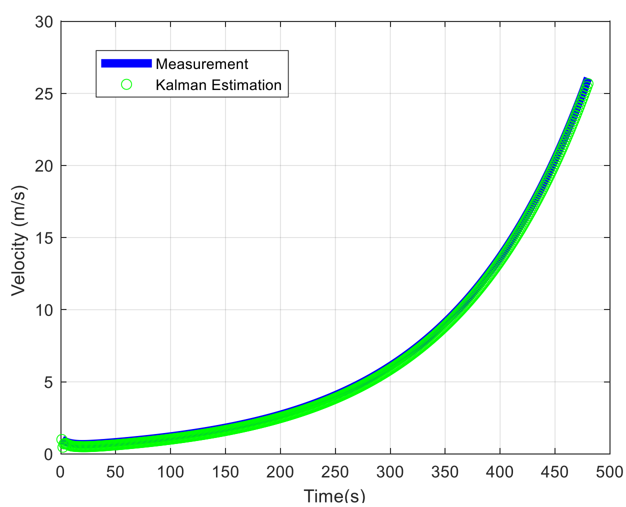

Figure 7. SDI33 IMU X-axis Velocity, +20°C

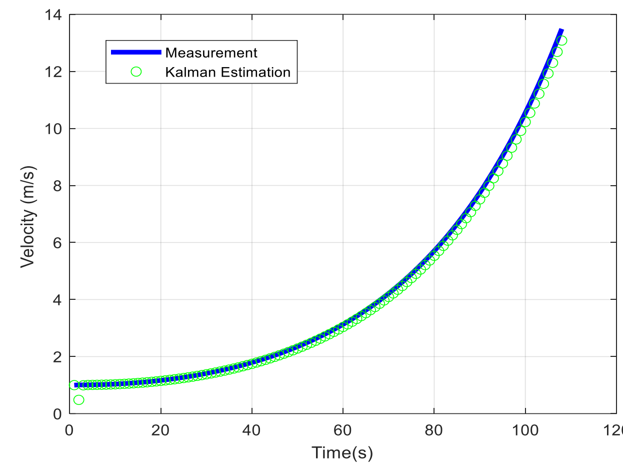

Figure 8. HG9900C1A IMU X-axis velocity, +20°C

At the beginning of the study, we designed a Kalman filter using a linear model to check the accuracy of the algorithm we developed in MATLAB. The speed values we obtained by processing the data we received for both IMU sensors and the speed estimated by the Kalman filter are shown in Figure 7 and Figure 8. These figures show that the measured and estimated speed values are close to each other in the measurements taken at room temperature, and although they do not completely overlap, there are occasional deviations.

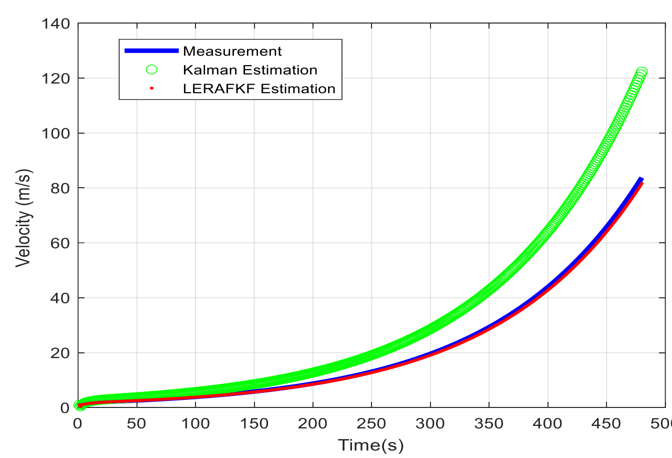

Figure 9. SDI33 IMU X-axis Velocity (Incorrect State–Space Model), +20°C

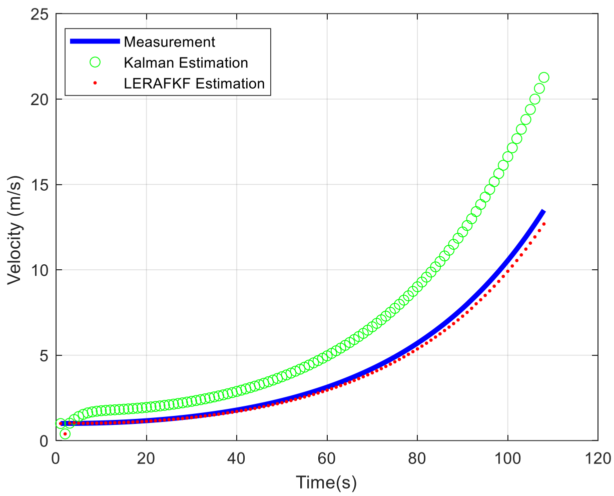

Figure 10. HG9900C1A IMU X-axis Velocity (Incorrect State-Space Model), +20°C

In the second part, we examined the prediction performance of the Kalman Filter and our proposed filter when we used the wrong state space model at a constant temperature of +20°C. After validating our Kalman filter algorithm, we used a linear system model with imperfect measurement parameters. Using this imperfect model, we compared the estimation performances of the Kalman filter and LERAFKF algorithms. The Kalman filter estimates of the X-axis velocities compared with the measurements are shown in Figure 9 and Figure 10. As shown in these figures, the estimation performance of the Kalman filter deteriorates, and divergence occurs as time increases. On the other hand, the LERAFKF estimates follow the measurements well. The regression analysis at +20°C for the incorrectly constructed state-space model of the LERAFKF and the Kalman filter is given in Table 3. Here, Maen Square Error (MSE) values indicate that that the LERAFKF predictions are better than those of the KF.

Table 3. MSE values comparison of KF and LERAFKF Estimates

Regression Analysis Results With Average Square Error , +20°C	Velocity Estimation Methods	
	KF	LERAFKF
SDI33 IMU Sensor	2.238	0.251
HG9900C1A IMU Sensor	1.917	0.084

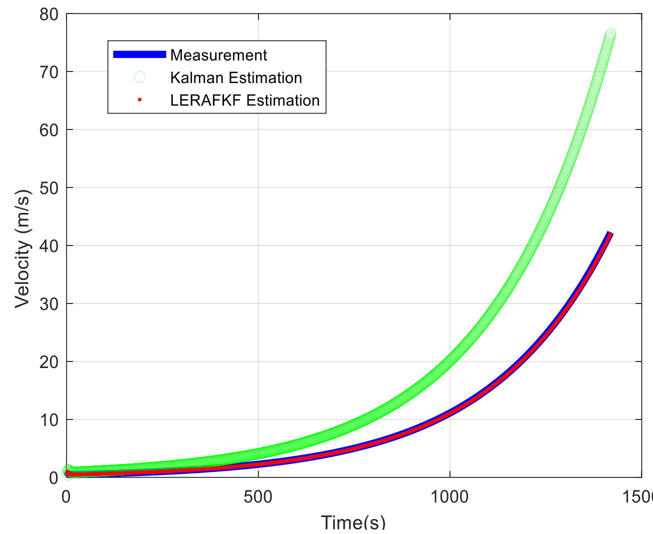

Figure 11. SDI33 IMU X-axis velocity (incorrect state-space model), -20°C -+50°C

In the third study, the performances of the KF and LERAFKF prediction algorithms are tested at different temperature ranges. The temperature of the experimental environment was increased from -20°C to +50°C, and the sensor characteristics were examined.

The sensor characteristics presented in Table 1 and Table 2 coincide with our findings that the HG9900C1A sensor is more stable than the SDI33 sensor in terms of measurement accuracy against temperature changes.

In summary, we examined the prediction performance of the Kalman filter and LERAFKF when we used the wrong state space model due to temperature changes. The resulting simulation studies are shown in Figure 11 and Figure 12. The Kalman filter estimate drifts away from the measured values as time passes, while the LERAFKF estimates follow the measurements well. The regression analysis for the prediction performance of the SDI33 and HG9900C1A IMU sensors against temperature change is given in Table 4. Considering the MSE values, we see that the LERAFKF predictions are better than those of the KF.

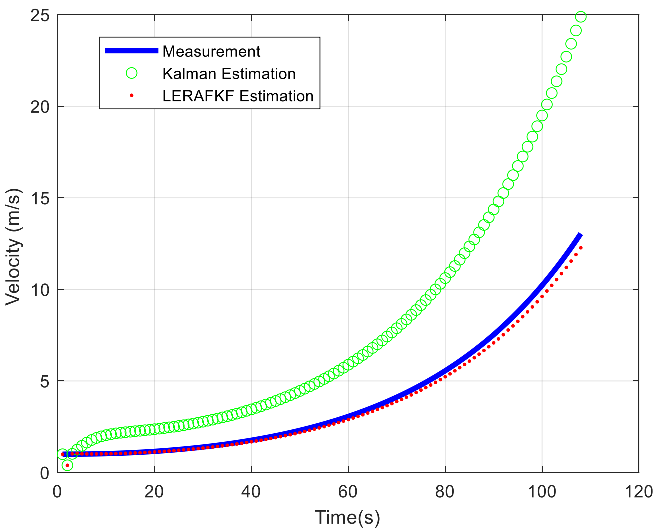

Figure 12. HG9900C1A IMU X-axis velocity (incorrect state-space model), -20°C -+50°C

Table 4. MSE values comparison of KF and LERAFKF Estimates

Regression Analysis Results With Average Square Error, -20°C - +50°C	Velocity Estimation Methods	
	KF	LERAFKF
SDI33 IMU Sensor	3.058	0.843
HG9900C1A IMU Sensor	2.531	0.272

We compared the performance of LERAFKF with that of several similar studies in the literature. The comparisons show that LERAFKF provides better prediction performance than do the other methods. In a study on speed estimation, Feng Y. et al. [25] conducted a study on speed estimation. We compared the prediction results of the LERAFKF with those of their proposed strong tracking Kalman filter (STKF). Another study by Fakharian A. et al. [27] compared a conventional Kalman filter with an adaptive Kalman filter (AKF). The results of the estimation in terms of the MSE values are provided in Table 5. Here, KF stands for the conventional Kalman filter, and the adaptive Kalman filter is used for the adaptive filters (STKF, AKF, and LERAFKF). When we compare the LERAFKF performance in terms of the MSE, we observe that the LERAFKF outperforms these two proposed algorithms.

Table 5. Performance Comparison of the Velocity Estimation

Estimation Method (Regression Analysis with MSE)	Velocity Estimation Methods	
	KF	AFKF
Feng Y. et al [25]	1.4882	0.2743
Fakharian A. et al [27]	3.54	0.12
In Our Study	1.917	0.084

5. Conclusion

Inertial navigation systems are used in the foreground due to their independent operation in positioning systems. Position, orientation and velocity information can be measured by using accelerometers and gyroscope sensors in these systems. In the studies conducted to date, Kalman filter algorithms have been generally used in velocity estimation for linear systems.

In GNSS-INS integrated navigation applications, when the GNSS is disabled, deviations occur in the prediction values of the Kalman filter as a result of incorrect establishment of the state-space model due to cumulative accumulated errors in the INS and measurement-related errors depending on the sensor temperature, and in such cases, the Kalman filter loses its success.

In our test environment, acceleration measurements were taken at 3 different temperatures (+20°C, -20°C, +50°C) using an IMU in an environment where a moving object was simulated for linear systems. For this purpose, a multifeature HG9900C1A IMU system with 9 degrees of freedom was used. This system is a special system used to simulate missiles. Acceleration measurements were made with the IMU integrated into the system. These measurements were input to our algorithms designed in the MATLAB environment, and the prediction algorithms of both the KF and LERAFKF filters were tested. Detailed studies were carried out with measurements taken from test environments established on the algorithms we developed in the MATLAB environment. In these studies, the performance of the KF was compared with that of the LERFAFKF. Considering the results obtained, it can be seen that the LERAFKF algorithm has better performance than the KF algorithm against erroneous measurements caused by temperature changes. However, the performance of the LERAFKF algorithm increases with time, and in the initial stages, the LERAFKF algorithm achieves the same prediction performance as the other algorithms. Regression analyses also prove that LERAFKF in long-range navigation applications provides robust state estimates of measurement errors despite variations in sensor temperature. Considering the results obtained, it can be seen that the proposed LERAFKF algorithm outperforms the KF algorithm against inaccurate measurements due to temperature changes. This feature ensures satisfactory estimates in real life without having to use very expensive sensors.

Here, it would not be correct to say that LERAFKF is not affected by temperature changes at all. It would be more accurate to say that LERAFKF is more robust to temperature changes than the KF algorithm.

Nomenclature

INS	: Inertial Navigation System
MEMS	: Microelectronic Mmechanical System
KF	: Kalman Filter
GNSS	: Global Navigation Satellite System
IMU	: Inertial Measurement Unit
GPS	: Global Positioning System
LERAFKF	: Low Error Rate Adaptive Fading Kalman filter
AKF	: Adaptive Kalman Filter
STKF	: Strong Tracking Kalman Filter
MSE	: Mean Square Error
GPS	: Global Positioning System

Conflict of Interest Statement

The authors declare that there is no conflict of interest in the study.

References

[1] Toda A, Koike Y. Simulation Design of Thermopile and Magnetometer Aided INS/GPS Navigation System for UAV Navigation. Presented at International Symposium on Inertial Sensors and System;2021;http://doi.org/10.1109/INERTIAL51137.2021.9430487.

[2] Titterton D. H. and Weston, J. L. Strapdown Inertial Navigation Technology. Journal of American Institute of Aeronautics and Astronautics, 2004 ; https://doi.org/10.1049/ PBRA017E.

[3] Tan C.M., Wang, Y., Zhu X.H., Su Y., Wei G. Improved Alignment Method for a SINS Using Two Vector Measurements. Presented at the 5th International Conference on Instrumentation and Measurement, Computer, Communication and Control (IMCCC);2015; Qinhuangdao, China.

[4] Xile G, Haiyong L, Bokun N, Fang Z, Linfeng B, Yilin G, Yiming X, Jingang J. RL-AKF : An Adaptive Kalman Filter Navigation Algorithm Based on Reinforcement Learning for Ground Vehicles. Journal of Remote Sensing. 2020; 12 ; 1704. https://doi.org/10.3390 /rs12111704.

[5] Kalman, R. E. A New Approach to Linear Filtering and Prediction Problems. Journal of Basic Engineering. 1960; 82; 35-45.

[6] Mehra R.K. Identification Of Stochastic Linear Dynamic Systems Using Kalman Filter Representation. Journal of AIAA. 1971; 9(1); 28-31. https://doi.org/10.2514/3.6120.

[7] Lee T.S. Theory And Application Of Adaptive Fading Memory Kalman Filters, Journal of IEEE Transactions on Circuits and Systems. 1988; 35 (4) ; 474–477. https://doi.org/ 10.1109/31.1769.

[8] Xia Q, Shen X. Adaptive Fading Kalman Filter with an Applications. Journal of Automatica. 1998; 34(12); 1663-1664.

[9] Bar-Shalom Y, Li X.R, Kirubarajan T. Estimation with Applications to Tracking and Navigation. Journal of Computer Science, 2022; 1, https ://doi.org/10.1002/0471221279.ch11.

[10] Hide C, Moore T, Smith M. Adaptive Kalman Filtering For Low-Cost INS/GPS, Journal of Navigation, 2003; 56(1);143-152, https://doi.org/10.1017/S0373463302002151.

[11] El-Sheimy N, Hou H, Niu X. Analysis And Modelling Of Inertial Sensors Using Allan Variance, Journal of IEEE Trans. Instrum. Meas. 2008; 57(1); 140-149. https://doi.org/10.1109/ TIM.2007.908635.

[12] Ding W, Wang J, Rixos C, Kinlyside D. Improving Adaptive Kalman Estimation in GPS/INS Integration, The Journal of Navigation. 2007; 60(3); 517–529. https://doi.org/ 10.1017/ S0373463307004316.

[13] Gao B, Hu G, Yongmin Z, Xinhe Z. Cubature Kalman Filter with Both Adaptability and Robustness for Tightly Coupled GNSS/INS Integration. Journal of IEEE Sensors. 2021;21(1); 99-105. https://doi.org/ 10.1109/ JSEN.2021.3073963.

[14] Song J, No H, Kim J, Bae Y, Kee C. Performance Enhancement and Countermeasure for GPS Failure of GPS/INS Navigation System of UAV Through Integration of 3D Magnetic Vector. Journal of Positioning, Navigation, and Timing Performance. 2018; 7(3); 155-163. https://doi.org/10.11003/ JPNT.2018.7.3.155.

[15] Zhang L, Wang S, Neusyoina M. S, Konstantin A. New Adaptive Kalman Filter For Navigation Systems Of Carrier-Based Aircraft. Chinese Journal of Aeronautics. 2021;35(1). https://doi.org/ 10.1016/ /j.cja.2021.04.014.

[16] Faragher R, Understanding the Basis of the Kalman Filter Via a Simple and Intuitive Derivation. IEEE Signal Processing Magazine. 2012; 29(5);128-132. https://doi.org/ 10.1109/ MSP.2012.2203621.

[17] Bou S, Zhenwei Z, Shicai L, Xiaobing Y, Chengxu Y. Integrated Navigation Algorithm Based on Multiple Fading Factors Kalman Filter. Journal of IEEE Sensors. 2022; 22(14);1-18. https://doi.org/10.3390/ s22145081.

[18] Akbaş EM, Çifdalöz O, Üçüncü M. Improving the performance of a MEMS-IMU system based on a false state-space model by using a fading factor adaptive Kalman filter. Measurement and Control. 2024;0(0). https://doi.org/10.1177/00202940241258.

[19] Ozbek L, Babacan E.K, Efe M, Stochastic Stability Of The Discrete-Time Constrained Extended Kalman Filter. Turkish Journal of Electrical Engineering & Computer Sciences, 2010; 18(2) ; 211-223, 2010. https://doi.org/10.3906/elk-0812-17.

[20] Zarchan P, Musoff H. Fundamentals of Kalman Filtering. A Practical Approach, 2nd Edition, 2013.

[21] Kozlov A.V, Tarygin I.E, Golovan A.A. Calibration of inertial measurement units on a low-grade turntable with simultaneous estimation of temperature coefficients. Presented at 21 st St. Petersburg International Conference on Integrated Navigation Systems; 2014; St. Petersburg. Russia.

[22] Hu P, Chen B, Zhang C, Wu Q. Correlation-Averaging Methods and Kalman Filter Based Parameter Identification for a Rotational Inertial Navigation System. IEEE Trans. Industrial Informatics. 2018; 3(15); 1321–1328. https://doi.org/10.1109/ TII.2018.2850756.

[23] Hashlamon I, Erbatur K. An Improved Real-Time Adaptive Kalman Filter With Recursive Noise Covariance Updating Rules.

Turkish Journal of Electrical Engineering and Computer Sciences. 2016; 24(2); 524-540. https://doi.org/10.3906/elk-1309-60.

[24]Ozbek L, Efe M. Fading Kalman Filter For Manoeuvring Target Tracking. Journal of the Turkish Statistical Association. 1999; 2(3); 193–206.

[25]Feng Y, Li X., Zhang X. An adaptive compensation algorithm for temperature drift of microelectromechanical systems gyroscopes using a strong tracking Kalman filter. Journal of Sensors. 2015; 15(5); 11222-11238. https://doi.org/10.3390/ s150511222.

[26]Orderud F, Saelands S. Comparison of Kalman Filter Estimation Approaches for State Space Models with Nonlinear Measurements. Journal of Engineering and Mathematics. 2005.

[27]Fakharian A, Thomas M. Adaptive Adjustment of Noise Covariance in Kalman Filter for Dynamic State Estimation. Presented at 11 th International Conference on Networking, Sensing and Control. 2025; Oulu, Finland.